Molecular Biology of the Cell
Vol. 11, 1875–1886, May 2000

Involvement of a Small GTP-binding Protein (G Protein) Regulator, Small G Protein GDP Dissociation Stimulator, in Antiapoptotic Cell Survival Signaling

Ayumi Takakura,* Jun Miyoshi,* Hiroyoshi Ishizaki,* Miki Tanaka,* Atsushi Togawa,* Yasuko Nishizawa,† Hisahiro Yoshida,‡ Shin-ichi Nishikawa,‡ and Yoshimi Takai*§‖

*Takai Biotimer Project, Exploratory Research in Advanced Technology, Japan Science and Technology Corporation, c/o JCR Pharmaceuticals, Kobe 651-2241, Japan; †Department of Experimental Pathology, Osaka Medical Center for Cancer and Cardiovascular Diseases, Osaka 537-8511, Japan; ‡Department of Molecular Genetics, Faculty of Medicine, Kyoto University, Kyoto 606-8502, Japan; and §Department of Molecular Biology and Biochemistry, Osaka University Graduate School of Medicine/Faculty of Medicine, Osaka 565-0871, Japan

Submitted September 17, 1999; Revised January 18, 2000; Accepted March 8, 2000
Monitoring Editor: Martin Schwartz

Small GTP-binding protein GDP dissociation stimulator (Smg GDS) regulates GDP/GTP exchange reaction of Ki-Ras and the Rho and Rap1 family members and inhibits their binding to membranes. In fibroblasts, Smg GDS shows mitogenic and transforming activities in cooperation with Ki-Ras. However, the physiological function of Smg GDS remains unknown. Here we show that mice lacking Smg GDS died of heart failure shortly after birth, not resulting from developmental heart defects but from enhanced apoptosis of cardiomyocytes triggered by cardiovascular overload. Furthermore, neonatal thymocytes and developing neuronal cells underwent apoptotic cell death. Smg GDS−/− thymocytes were susceptible to apoptotic inducers, such as etoposide and UV irradiation. Smg GDS−/− thymocytes were protected from etoposide-induced cell death by ex vivo transduction of the Smg GDS cDNA. These phenotypes partly coincide with those observed in Ki-Ras-deficient mice, suggesting that Smg GDS is involved in antiapoptotic cell survival signaling through Ki-Ras.

INTRODUCTION

Small GTP-binding proteins (G proteins) consist of the five families: the Ras, Rho, Rab, Arf/Sar, and Ran families (Bourne *et al.*, 1990, 1991; Hall, 1990; Takai *et al.*, 1992). The Ras family mainly regulates gene expression; the Rho family mainly regulates the cytoskeleton and gene expression; the Rab and Arf/Sar families regulate vesicle trafficking; and the Ran family regulates transport between the cytosol and the nucleus. Thus, the functions of the many small G proteins have been clarified, but it remains unknown how and when individual members of the superfamily interact with and exchange signals to efficiently regulate multicellular functions.

We have attempted to down-regulate the activity of small G proteins by disrupting their regulators. Small G proteins serve as a molecular switch for transducing signals by exchanging the GTP- and GDP-bound states. Three types of regulators have been identified: they are guanine-nucleotide exchange proteins (GEPs), GDP dissociation inhibitors (GDIs), and GTPase-activating proteins. GEPs convert the GDP-bound inactive form to the GTP-bound active form by stimulating the dissociation of GDP from the GDP-bound form; GDIs inhibit the GEP-induced conversion from the GDP-bound form to the GTP-bound form by inhibiting the dissociation of GDP from the GDP-bound form; and GTPase-activating proteins convert the GTP-bound form to the GDP-bound form by stimulating the GTPase activity (Takai *et al.*, 1993). Although these regulators are required to

‖ Corresponding author. E-mail address: ytakai@molbio.med.osaka-u.ac.jp.

Abbreviations used: BrdU, bromodeoxyuridine; dpc, days postcoitum; EGFP, enhanced green fluorescent protein; E, embryonic day; ES, embryonic stem; GDI, guanine-nucleotide dissociation inhibitor; GDS, guanine-nucleotide dissociation stimulator; GEP, guanine-nucleotide exchange protein; G protein, GTP-binding protein; HE, hematoxylin and eosin; P, postnatal day; RT, reverse transcriptase; MLC, myosin light chain: TUNEL, terminal deoxynucleotidyl transferase–mediated dUTP nick end labeling.

enhance the efficiency of small G protein-mediated signaling, they are not always essential for viability of knockout mice. We have successfully generated mice lacking Rho GDIα (Togawa *et al.*, 1999) and found that deficiency of this protein leads to a less-deleterious phenotype than deficiency of its substrate small G protein itself. Indeed, this is also the case for deficiency of small G protein GDP dissociation stimulator (Smg GDS).

Smg GDS is the fourth type of regulator for small G proteins. This regulator was originally purified from bovine brain cytosol as a regulator of Rap1B (Yamamoto *et al.*, 1990). We subsequently isolated the bovine and human Smg GDS cDNAs and determined their nucleotide and amino acid sequences (Kaibuchi *et al.*, 1991; Kikuchi *et al.*, 1992). In a cell-free system using purified samples, Smg GDS stimulates the dissociation of GDP from a group of small G proteins including not only Rap1B but also Ki-Ras and the Rho, Rac, and Cdc42 subfamilies but is inactive on Ha-Ras (Mizuno *et al.*, 1991; Ando *et al.*, 1992; Hiraoka *et al.*, 1992; Yaku *et al.*, 1994). This substrate specificity is different from that of other GEPs, such as *son of sevenless* (Simon *et al.*, 1991) and Cdc25 (Jones *et al.*, 1991) for the Ras subfamily and C3G (Gotoh *et al.*, 1995) and Epac/cAMP guanine-nucleotide exchange factor (de Rooij *et al.*, 1998; Kawasaki *et al.*, 1998) for the Rap subfamily, but is similar to those of GDIs, such as Rho GDI (Takai *et al.*, 1993) and Rab GDI (Takai *et al.*, 1993). In intact NIH3T3 cells, Smg GDS shows transforming activity in cooperation with Ki-Ras (Fujioka *et al.*, 1992), and in Swiss 3T3 cells it shows mitogenic activity in cooperation with Ki-Ras or Rap1 (Yoshida *et al.*, 1992), suggesting that Smg GDS functions as a stimulatory regulator for these small G proteins in intact cells as described for Cdc25 and *son of sevenless* (Crechet *et al.*, 1990; Hughes *et al.*, 1990; Bonfini *et al.*, 1992). However, the physiological function of Smg GDS remains to be established.

In this study, we report that Smg GDS deficiency in mice results in enhanced apoptosis in a variety of cell types, including cardiomyocytes, thymocytes, and neuronal cells, and that these phenotypes are correlated with those of Ki-Ras-deficient mice, suggesting that Smg GDS regulates at least antiapoptotic cell survival signaling presumably through Ki-Ras.

MATERIALS AND METHODS

DNA Library Screening

The Smg GDS cDNA was isolated from mouse brain cDNA library λ TriplEx (Clontech, Palo Alto, CA) using the bacterial strains and the manufacturer's protocol and sequenced using an Applied Biosystems (Foster City, CA) DNA sequencer. A cDNA fragment encoding the N-terminal half-region of Smg GDS was subcloned into appropriate plasmid vectors and used as a probe for homology screening of 129SVJ mouse genomic library λ FIXII (Stratagene, La Jolla, CA).

Generation of Smg GDS−/− Mice

A targeting construct was made to replace 3′ half of the coding exon 5 and the following exons 6 and 7 (amino acids 212–343 of the Smg GDS protein) with a neo-resistance gene cassette. RW4 embryonic stem (ES) cells were transfected and selected as described (Togawa *et al.*, 1999). Homologous recombinants were verified by Southern hybridization using 5′ and 3′ external probes and the neo-resistance gene probe. Smg GDS+/− ES cells were microinjected into embryonic day 3.5 (E3.5) C57BL/6J blastocysts and transferred to MCH pseudopregnant foster mothers to generate chimeras that were mated with BDF1 mice for germ line transmission. Mice with mutant alleles were also back-crossed with C57Bl/6 mice. Genotyping was performed by Southern hybridization and PCR using primers in the neo gene (5′-CCGCTTGGGTGGAGAGGCTAT-3′ and 5′-TGGTGGTCGAATGGGCAGGTA-3′) and in the replaced Smg GDS gene (5′-TCCCCGCTATCTTCAGTATCT-3′ and 5′-GCACAGTATTCAAAACCATCC-3′). The PCR mixtures were denatured for 2 min at 95°C and annealed for 1 min at 55°C. PCR was performed 25 cycles as follows: extend for 2 min at 72°C, denature for 30 s at 95°C, and anneal for 1 min at 55°C. Samples were extended for an additional 5 min at 72°C. PCR products were visualized on 4% 3:1 NuSieve agarose (Takara, Berkeley, CA)-Tris acetate-EDTA gels.

Antibodies and Western Blot Analysis

An anti-Smg GDS antibody was prepared as described (Kikuchi *et al.*, 1992). Mouse brains were homogenized in a lysis buffer of 320 mM sucrose, 20 mM Tris-Cl, pH 7.5, 2 mM EDTA, and 10 mM PMSF. Fifty micrograms of proteins were separated by SDS-PAGE, transferred to an Immobilon membrane (Millipore, Bedford, MA), and blocked for 1 h in Tris-buffered saline containing 5% BSA. After incubation with the anti-Smg GDS antibody for 1 h and then with peroxidase-conjugated secondary antibody for 1 h, the blots were developed with ECL (Amersham Pharmacia Biotech, Uppsala, Sweden).

Reverse Transcriptase-PCR (RT-PCR)

Total RNA was extracted from mouse brains of each genotype using TRIzol reagent (Life Technologies, Gaithersburg, MD) and processed according to the manufacturer's protocol. First-strand cDNA was generated using Moloney reverse transcriptase and reagents supplied with the cDNA synthesis kit (Stratagene). To analyze expression of Smg GDS mRNA, 20% (4 μl) of the reaction was used in a 50-μl PCR amplification using 5 U of *Taq* DNA polymerase, 2 mM $MgCl_2$, 150 μM dNTPs, 1 μM primers (primer 1, 5′-AAGCTACTGGGCATTCACTGC-3′, and primer 2, 5′-TTTCTGCATGGACTCATCTCC-3′). PCR was performed for 25 cycles as follows: extend for 2 min at 72°C, denature for 30 s at 95°C, and anneal for 1 min at 55°C. Samples were extended for an additional 5 min at 72°C. PCR products were electrophoresed on 4% 3:1 Nusieve agarose (Takara) gels and analyzed by Southern hybridization using the Smg GDS cDNA probe. To analyze differentiation of cardiac muscles, RNA was prepared from embryonic hearts at 17.5 d postcoitum (dpc), and RT-PCR was performed as described (Lyons *et al.*, 1995) using primers 5′-ACACACTCTCTTCACCTGGC-3′ and 5′-ATGAAACTCCAAGCTGGGGC-3′ for myosin light chain 1A (MLC-1A), primers 5′-ATATCATGGCGAGCTGAGCC-3′ and 5′-AGAGTGACTGCAGGAGTCCG-3′ for MLC-1V, and primers 5′-TGTTCCTCACGATGTTTGGG-3′ and 5′-CTCAGTCCTTCTCTTCTCCG-3′ for MLC-2V.

Histological Analysis

Embryos and newborn mice were fixed in Bouin's solution or 4% paraformaldehyde, paraffin embedded, serially sectioned (5 μm), and stained with hematoxylin and eosin (HE). Terminal deoxynucleotidyl transferase–mediated dUTP nick end labeling (TUNEL) staining was performed on paraformaldehyde-fixed sections using an in situ apoptosis detection kit (Takara). Briefly, sections were incubated with proteinase K (20 μg/ml) for 15 min at 37°C, and then endogenous peroxidase was blocked by incubation in 3% H_2O_2. After washing with PBS, the TUNEL reaction mixture containing terminal deoxynucleotidyl transferase enzyme and labeling buffer was applied to the sections in a moist chamber and incubated for 75 min at 37°C. The sections were then washed three times in PBS, incubated with an anti-FITC HRP-conjugated antibody for 30 min,

rinsed twice, and visualized with 3,3′-diaminobenzidine tetrahydrochloride and H_2O_2. Finally, the sections were counterstained with hematoxylin. For in vivo bromodeoxyuridine (BrdU) labeling, BrdU (0.5 mg dissolved in 0.5 ml of saline per mouse) was injected intraperitoneally into pregnant females at 11.5 and 12.5 d of gestation. The females were killed 1 h after injection; the embryos were fixed in 4% paraformaldehyde at 4°C overnight and processed for immunohistochemistry as described (Fushiki *et al.*, 1997).

Induction of Apoptosis in Thymocytes Ex Vivo

Single-cell suspensions of neonatal thymi were washed twice in RPMI 1640 medium supplemented with 10% FCS treated with dextran-coated charcol and incubated for 30 min at 37°C in 5% CO_2 to remove endogenous glucocorticoids. Thymocytes were plated at 1×10^6/ml in 24-well tissue culture plates and treated with the following cell death stimuli: dexamethasone (Sigma, St. Louis, MO), etoposide (Clontech), anti-Fas antibody Jo2 (PharMingen, San Diego, CA) plus 30 μg/ml cycloheximide, and UV irradiation. Caspase-3 activity was measured using ApoAlert CPP32/Casp-3 fluorescent assay kit (Clontech). Cleavage of acetyl-aspartyl-glutamyl-valyl-aspart-1-aldehyde-7-amino-4-trifluoromethyl coumarin was measured by a fluorospectrophotometer (RF-1500; Shimadzu, Tokyo, Japan). Thymocytes were stained with propidium iodide (Sigma), annexin V (PharMingen), and antibodies against CD4 and CD8 and analyzed by a FACSVantage dual-laser flow cytometer (Becton-Dickinson, San Jose, CA).

Retrovirus-mediated Gene Transfer

The full-length Smg GDS cDNA and enhanced green fluorescent protein (EGFP) cDNA as a control were subcloned into pLNCX retroviral vector at the *Hpa*I site and transfected into PT96 cells to produce infectious recombinant retroviruses. Packaging cells were selected for 1 wk in the presence of G418 (500 μg/ml). Retroviral transduction was performed as described by the manufacturer's protocol (Clontech). Cell culture media containing 10^6–10^7 virus particles/ml were filtered through a 0.45-μm filter (Millipore) and added to 1×10^6 thymocytes for 24 h to allow expression of the genes. Thymocytes were then treated with etoposide to induce apoptosis.

RESULTS

Generation of Smg GDS−/− Mice

The mouse Smg GDS gene includes nine exons that encompass the translated region encoding 558 amino acids. Exon 9 encodes the functional domain located at the C-terminal fifth of Smg GDS (amino acid residues 442–492), whose mutations totally abolished in vitro GTP/GDP exchange activity on Ki-Ras, Rap1, and RhoA (Kotani *et al.*, 1992). Then we have generated Smg GDS+/− ES cells by homologous recombination using a targeting vector designed to delete 1.7 kb of genomic DNA containing the 3′ half of the coding exon 5 and the following exons 6 and 7 of the Smg GDS gene (Figure 1A). When the targeting construct was electroporated into ES cells, three G418-resistant colonies heterozygous for the Smg GDS gene were obtained. The genotypes of the G418-resistant colonies were confirmed by Southern blot analysis. These ES clones were used to generate chimeric mice and successfully contributed to germ line transmission. Smg GDS heterozygotes were intercrossed to produce homozygous mutant offspring (Figure 1, B and C). Mice homozygous for the disrupted allele expressed neither the intact Smg GDS protein as analyzed by immunoblots using an antibody specific for the C-terminal domain nor the RT-PCR product derived from the Smg GDS mRNA (Figure 1, D and E). Although there remains a possibility that exons 1–4 of the targeted allele could generate the N-terminal third portion of Smg GDS, such a truncated product would have lost the physiological role, because we have previously shown that the C-terminal domain is essentially required for Smg GDS activity (Kotani *et al.*, 1992). We conclude that this disruption results in mice that are functionally null for Smg GDS.

Requirement of Smg GDS for Neonatal Survival

Smg GDS heterozygous mice were viable with no detectable phenotype. In contrast, Smg GDS deficiency resulted in an unusual reduced rate of live Smg GDS−/− mice. In heterozygous intercrosses, homozygous mice were 7% of total mice at 3 wk of age, significantly lower than the expected ratio of 25% (Table 1). Genotyping of embryos showed no evidence of embryonic lethality, however, suggesting that Smg GDS is not essential for mouse development but is implicated in postnatal survival. We then determined the survival percent of Smg GDS−/− mice at 0–10 d after birth. Nearly 70% of Smg GDS−/− mice died within 5 d after birth (Figure 2A). These mice became weak at 0–2 d after birth (postnatal day 0 [P0]–P2) and tended to die within 20–30 h from the onset of symptoms. Approximately 30% of Smg GDS−/− mice survived the critical period. These surviving mice developed almost normally in an environment free of specific pathogens, and they were fertile and viable for >6 mo. Survival rates of second-generation Smg GDS−/− offspring were also nearly 30%, consistent with those observed in Smg GDS−/− mice arising from the initial heterozygous intercrosses (Figure 2B). Moreover, this survival tendency was conserved in the C57Bl/6 genetic background after three generations of back-crossing (our unpublished results). These findings indicate that Smg GDS−/− mice are at a significant survival disadvantage compared with wild-type and Smg GDS+/− littermates, and that such a property is genetically associated with Smg GDS deficiency.

Heart Failure in Smg GDS−/− Mice

We examined Smg GDS−/− mice at 1 d after birth on both macroscopic and microscopic levels. Approximately two-thirds of them showed signs of heart failure: cyanosis, edema, and decrease in turgor of the skin. The Smg GDS−/− heart was enlarged macroscopically as expected; the atrial, ventricular, and septal walls were extremely thin. Histologically, both the atrial and ventricular chambers were extended and associated with reduced trabeculation compared with matched wild-type littermates (Figure 3, Aa and Ba). Myocardium of the Smg GDS−/− heart showed markedly decreased cellularity but was not associated with infiltration of inflammatory cells (Figure 3, Ab and Bb). The liver and lungs of Smg GDS−/− mice gained weight, 1.2- to 1.5-fold greater than littermate controls, and showed the histology of marked congestion (our unpublished results). In contrast, one-third of Smg GDS−/− mice did not show significant pathological abnormalities of the heart. Taken together, we conclude that neonatal death observed in 70% of Smg GDS−/− mice is caused by heart failure. These morphological changes of the Smg GDS−/− heart appeared

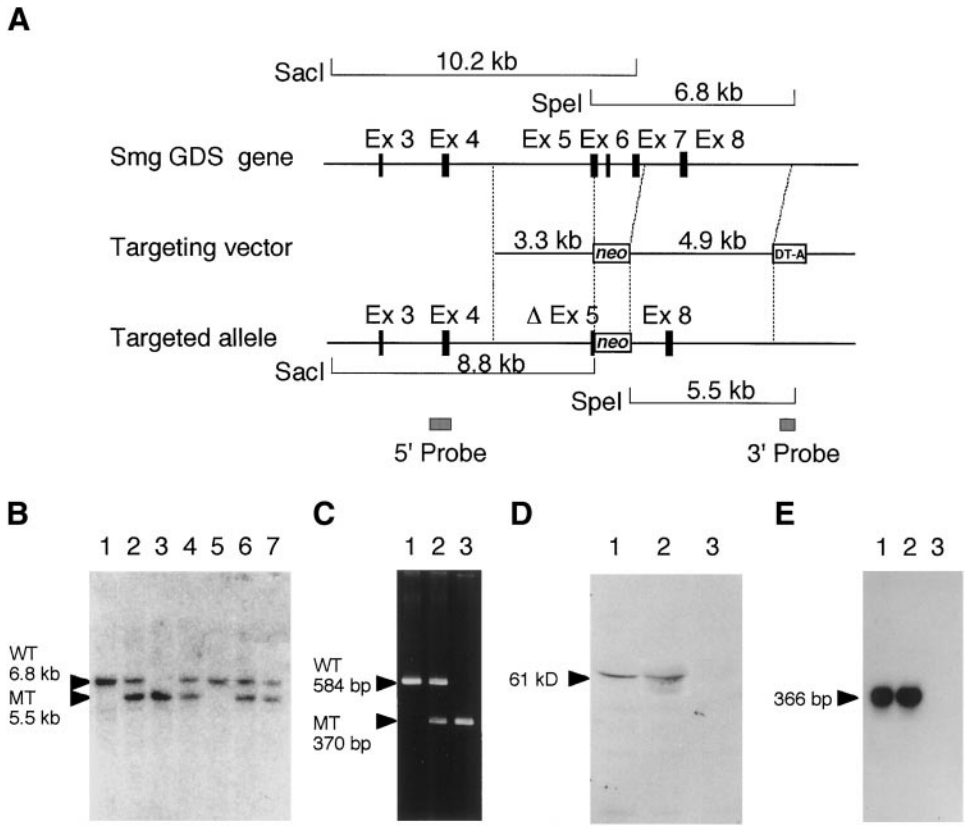

Figure 1. Targeted disruption of the Smg GDS gene. (A) Structure of the mouse Smg GDS gene with coding exons 3–8 is shown at the top. A targeting vector was designed to remove part of the exon 5 and the following exons 6 and 7. The construct contained 3.3-kb 5′ flanking sequences and 4.9-kb 3′ flanking sequences. The MC1-neo cassette was inserted at the *Pst*I site within exon 5, but the 5′ splice acceptor site was kept intact. The diphtheria toxin A cassette was inserted at the 3′ end. In the targeted allele, the MC1-neo cassette replaces 1.7 kb of the genomic DNA region. Homologous recombination was verified by using informative restriction fragments and diagnostic probes as indicated. (B) Southern hybridization using *Spe*I-digested DNA extracted from mouse tails and the 3′ external probe shown in A. Mouse genotype was identified by the 6.8-kb wild-type (WT) and the 5.5-kb mutant (MT) fragments. Lanes 1 and 5, wild-type mice; lanes 2, 4, 6, and 7, Smg GDS+/− mice; lane 3, Smg GDS−/− mouse. (C) Genotyping by PCR analysis of DNA extracted from littermate mice at 21 d of age. PCR primers were selected to generate a 584-bp DNA product indicative of the wild-type (WT) allele or a 370-bp product attributable to the targeted (MT) Smg GDS allele. Lane 1, wild-type mouse; lane 2, Smg GDS+/− mouse; lane 3, Smg GDS−/− mouse. (D) Western blot analysis of proteins extracted from the brain of each genotype. The 61-kDa band of the Smg GDS protein was detected. Lane 1, wild-type mouse; lane 2, Smg GDS+/− mouse; lane 3, Smg GDS−/− mouse. (E) RT-PCR analysis using intron-spanning primers located in exons 5 and 7 and the Smg GDS mRNA from the brain of each genotype. The 366-bp band was amplified by Smg GDS-specific primers. Lane 1, wild-type mouse; lane 2, Smg GDS+/− mouse; lane 3; Smg GDS−/− mouse.

very similar to those of the Ki-Ras−/− heart (Koera *et al.*, 1997).

Apoptosis in Smg GDS−/− Cardiomyocytes

We asked whether the hypocellularity and abnormal architecture of the Smg GDS−/− heart would be due to diminished proliferative potential or enhanced apoptosis. In fact, the Ras/MAPK pathway has been thought for a long time to be involved in cell proliferation by mediating mitogenic signals (Buday and Downward, 1993; Egan *et al.*, 1993; Liu *et al.*, 1993; Vojtek *et al.*, 1993), but it has recently been shown that Ras mediates cell survival signaling in invertebrates (Bergmann *et al.*, 1998a,b; Kurada and White, 1998) and the murine hematopoietic cell line BaF3 (Walker *et al.*, 1998). To address the possibility that increased apoptosis in cardiomyocytes would lead to the thinning of atrial, ventricular, and septal walls of the Smg GDS−/− heart at 1 d after birth, we examined the hearts of E18.5 embryos and P0 neonatal mice using TUNEL staining, because apoptotic cells might have been processed and disappeared by 1 d after birth. Serial sections of HE and TUNEL staining were compared with visualize apoptotic cells between Smg GDS−/− mice and littermate controls. Although few pyknotic nuclei and TUNEL-positive cells were observed in cardiomyocytes of control and Smg GDS−/− embryos at 18.5 dpc (our unpublished results), massive cell death was found in the TUNEL staining of the Smg GDS−/− heart at the day of birth, namely 6 h after birth, compared with Smg GDS+/− littermate controls (Figure 3, Ca and Da). Degenerative changes were dominant at the endocardium of the left ventricle

Table 1. Genotyping of live mice arising from Smg GDS heterozygous crosses

	Genotype of Smg GDS-deficient mice		
Stage	+/+ (%)	+/− (%)	−/− (%)
E12.5	9/43 (21)	20/43 (47)	14/43 (32)
E13.5	19/65 (29)	26/65 (40)	20/65 (31)
E18.5	19/64 (30)	29/64 (45)	16/64 (25)
P0–P7	44/143 (31)	89/143 (62)	10/143 (7)
P21	75/270 (28)	177/270 (66)	18/270 (7)

Genotype of Smg GDS-deficient mice is indicated as +/+, +/−, and −/−. Genotyping was performed by Southern hybridization or PCR analysis at the ages indicated.

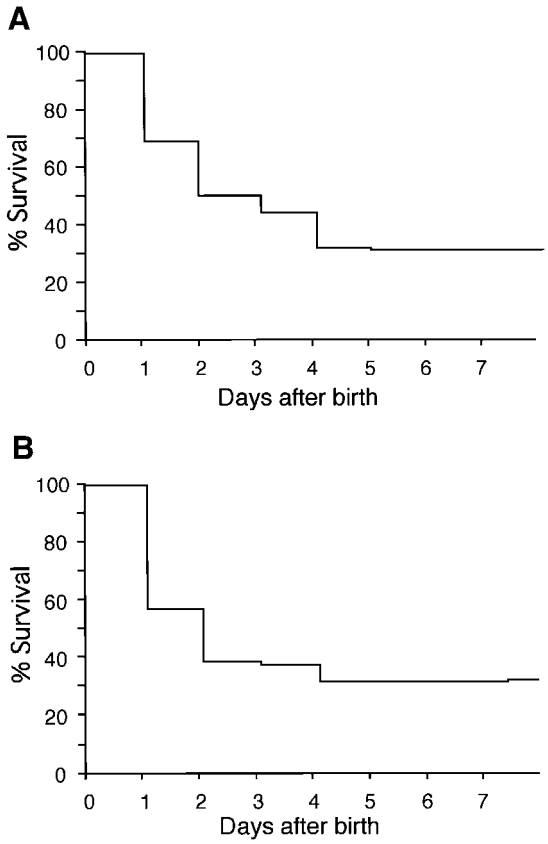

Figure 2. Life span of Smg GDS−/− mice. (A) Percent survival of first-generation Smg GDS−/− mice derived from heterozygote intercrosses (n = 274). (B) Percent Survival of second-generation Smg GDS−/− mice derived from homozygote intercrosses (n = 42). The results were similar in the 129/BDF and 129/C57BL genetic background (our unpublished results).

(Figure 3, Dc and Dd), leading to detachment of cardiomyocytes and dilatation of the ventricular chambers. It is intriguing that apoptotic cells were found in both ventricles of the Smg GDS−/− heart, whereas they were localized exclusively in the right ventricle of the Smg GDS+/− heart (Figure 3, Cb and Db) and wild-type control (our unpublished results). These findings suggest that apoptosis at the right side of the heart is part of a physiological process, reflecting the pressure overload caused by cardiovascular crisis during neonatal period.

We then tested proliferation of embryonic cardiomyocytes in vivo, because cardiac lesions in Ki-Ras−/− mice were observed at 13.5–15.5 dpc and considered to be caused by defective proliferation of heart muscle. Pregnant mice harboring embryos at 11.5 dpc were injected intraperitoneally with BrdU, and incorporation of BrdU into embryonal tissues was assessed histochemically. Heart sections showed no obvious differences by HE staining (Figure 4, Aa and Ba) between Smg GDS−/− mice and controls. Quantitative comparison of S phase nuclei (BrdU-positive) relative to the total number of cardiomyocyte nuclei in Smg GDS+/− and Smg GDS−/− hearts (data compiled from examining 32 sections from four embryos) revealed the rate of 22.2 ± 3.3% for Smg GDS+/− hearts and 21.3 ± 3.7% for Smg GDS−/− hearts, demonstrating that BrdU was incorporated at almost similar levels in both the Smg GDS−/− and control heart (Figure 4, Ab and Bb). To further analyze differentiation of cardiac muscles, we have isolated mRNA from embryonic hearts at 17.5 dpc and performed RT-PCR for detecting expression of the MLC-1A, -1V, and -2V genes (Figure 4C). There was no difference among the levels of RT-PCR products obtained from Smg GDS+/− and Smg GDS−/− hearts. These findings were consistent with those of immunostaining using an antibody against MLC-2V (our unpublished results). Finally, we analyzed primary cultures of embryonic cardiomyocytes at 13.5, 14.5, and 16.5 dpc but failed to detect any alterations in the organization of α-actinin into sarcomeric units, a marker of cardiomyocyte maturation (our unpublished results). These results indicate that cardiomyocytes proliferate and differentiate normally during embryogenesis of Smg GDS−/− mice, consistent with the mendelian genotype profiles of embryos arising from Smg GDS heterozygous intercroses.

Apoptosis in Neonatal Thymocytes and Developing Neuronal Cells in Smg GDS−/− Mice

In addition to the cardiac lesion, we found that thymi from Smg GDS−/− mice at 1 d after birth were markedly smaller than those of wild-type or Smg GDS+/− littermate controls with total thymocyte numbers reduced ~5- to 10-fold. Histological sections of Smg GDS−/− thymi exhibited widespread distribution of pyknotic nuclei with conserved structures of cortex and medulla (Figure 5, Aa, Ab, Ba, and Bb). Because abundant pyknotic nuclei are indicative for apoptosis, we performed TUNEL staining and found that apoptotic thymocytes were indeed increased in the Smg GDS−/− thymus (Figure 5, Ac and Bc). To confirm whether Smg GDS deficiency leads to a block in thymocyte maturation, Smg GDS−/− thymocytes were analyzed by flow cytometry. Nonetheless, profiles of CD4- and CD8-positive cell population were within normal limits (our unpublished results), suggesting that Smg GDS is not essentially required for T-cell differentiation.

Northern blot analysis revealed that the Smg GDS mRNA is expressed predominantly in the brain, and in situ hybridization analysis showed that Smg GDS transcripts are expressed in the medulla oblongata, the trigeminal ganglia, and the dorsal root ganglia of embryos at 18.5 dpc (our unpublished results). Additionally, elevated levels of apoptosis occurred in Ki-Ras-deficient mice during embryonic neurodevelopment (Koera *et al.*, 1997). To determine whether the effects of Smg GDS deficiency on neurogenesis could be explained in the context of functional association with Ki-Ras, we assayed for potential central nervous system lesions in Smg GDS−/− embryos. Although no gross structural abnormalities were observed in the Smg GDS−/− brain, pyknotic nuclei were found in the medulla oblongata (Figure 5Ca) and the spinal cord at 12.5 dpc. We then performed TUNEL staining to compare the extent of cell death and found that apoptotic cells were increased in the medulla oblongata (Figure 5, Cb and Cc), the trigeminal ganglia, the spinal cord, and the dorsal root ganglia compared with littermate controls (Figure 5, D–F). Because significant levels of apoptosis are believed to be essential for determining the

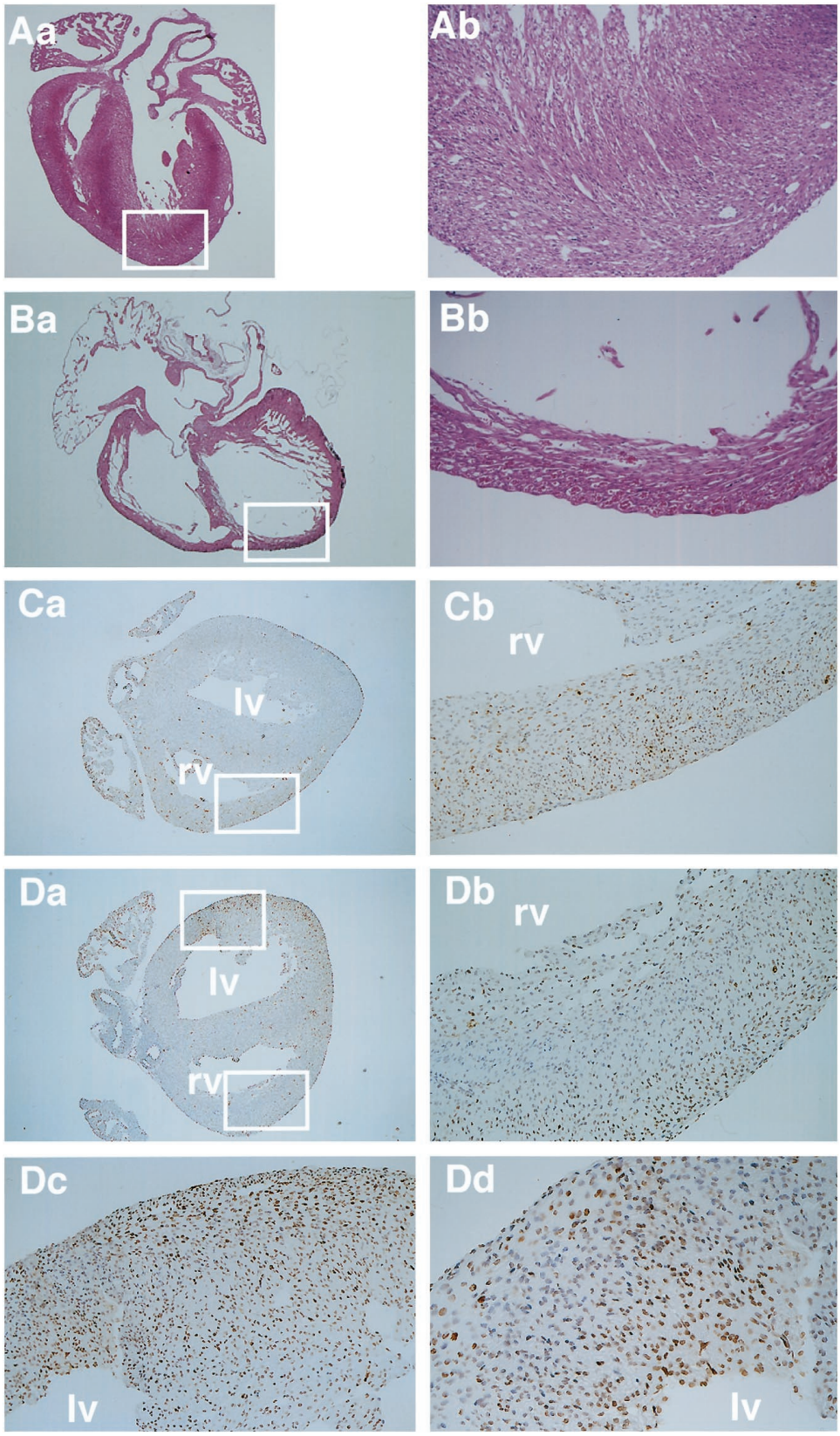

Figure 3. Histology of heart sections of wild-type and Smg GDS−/− mice and enhanced apoptosis in the Smg GDS−/− heart. (Aa and Ba) Representative sagittal sections (20×) of the wild-type heart (Aa) and the Smg GDS−/− heart (Ba) stained with HE at 1 d after birth. The Smg GDS−/− heart was dilated and expanded with thinning of atrial, ventricular, and septal walls compared with the littermate control. (Ab and Bb) Left ventricular walls (boxed regions in Aa and Ba) of the wild-type heart (Ab) and the Smg GDS−/− heart (Bb) at high-power (200×) magnification. Cellularity of the cardiomyocyte was markedly reduced in the Smg GDS−/− heart. (Ca and Da) TUNEL staining of the Smg GDS+/− heart and the Smg GDS−/− heart. They were prepared from littermate mice. The Smg GDS−/− heart (20×; Da) at the day of birth showed conserved architecture compared with the wild-type heart (20×; Ca). Cellularity of Smg GDS−/− cardiomyocytes was not reduced in contrast to marked hypocellularity of cardiomyocytes at 1 d after birth, as shown in Ba and Bb. (Cb and Db) Middle-power (100×) magnification of the right ventricles of the Smg GDS+/− heart (Cb; boxed in Ca) and the Smg GDS−/− heart (Db; boxed in Da). Note that TUNEL-positive cells are localized exclusively at the right ventricle of the Smg GDS+/− heart, whereas TUNEL-positive cells are found in both ventricles of the Smg GDS−/− heart. (Dc and Dd) Middle-power (100×; Dc) and high-power (200×; Dd) magnification of the left ventricular wall (boxed in Da) of the Smg GDS−/− heart. Numerous apoptotic cardiomyocytes were readily detected in the endocardium of the Smg GDS−/− heart, whereas apoptotic cells were not found in the left ventricular wall of the Smg GDS+/− heart. lv and rv, left and right ventricles, respectively.

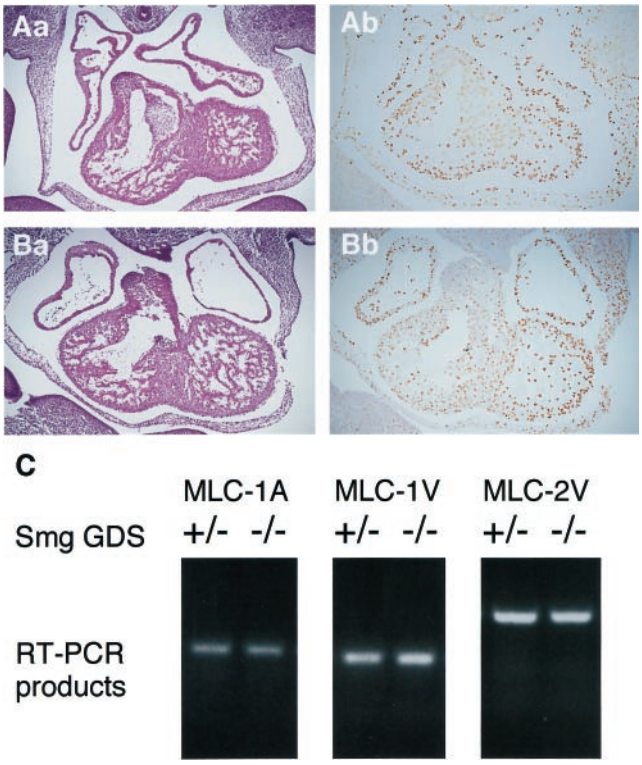

Figure 4. Normal proliferation and differentiation of cardiomyocytes in the Smg GDS−/− heart. Transverse sections through the heart of embryos at 11.5 dpc are shown. (Aa and Ba) HE staining of the Smg GDS+/− heart (Aa) and the Smg GDS−/− heart (Ba). (Ab and Bb) BrdU incorporation into proliferating cardiomyocytes was measured by immunohistochemical analysis. Sections of Smg GDS+/− (Ab) and Smg GDS−/− (Bb) embryos at 13.5 dpc were stained with a BrdU-specific antibody, and BrdU-positive cells per field were scored. (C) RT-PCR products derived from Smg GDS+/− and Smg GDS−/− heart mRNAs at 11.5 dpc were electrophoresed and stained with ethidium bromide. Primers were specific for the MLC-1A, -1V, and -2V genes.

cytoarchitecture of the brain, it is difficult to evaluate the pathological significance of these apoptotic changes, obviously incapable of causing embryonic lethality. On the other hand, we were unable to detect enhanced apoptosis in the fetal liver in which hematopoiesis was affected in Ki-Ras knockout mice (Johnson *et al.*, 1997). The result might be attributed to the difference of genetic background, because we used the same ES cell line and BDF mice for intercrossing as those of Koera *et al.* (1997) but not Johnson *et al.* (1997). It is notable, however, that the embryonic stages of these apoptotic neuronal cells and the distribution of apoptotic lesions in the nervous system coincide with those observed in Ki-Ras-deficient mice.

Apoptosis of Cultured Smg GDS−/− Thymocytes in Response to Etoposide and UV Irradiation

To study the relationship between Smg GDS deficiency and increased apoptosis, we used cultured Smg GDS−/− thymocytes that are more suitable than Smg GDS−/− cardiomyocytes and neuronal cells for a variety of apoptosis assays ex vivo. Smg GDS−/− and control thymocytes were isolated from newborn mice and challenged with four stimuli known to induce apoptosis. The extent of apoptosis was measured by cleavage activity of caspase-3, which is a direct upstream activator of deoxyribonucleases responsible for DNA fragmentation during apoptosis (Liu *et al.*, 1997; Enari *et al.*, 1998). Although dexamethasone and the anti-Fas antibody had no significant effect on Smg GDS−/− and control thymocytes (Figure 6, A and B), caspase-3 activity was increased three- to fourfold by etoposide and UV irradiation in Smg GDS−/− thymocytes compared with littermate controls (Figure 6, C and D). Because both the stimuli induce DNA damage response pathways (Lowe *et al.*, 1993a,b), Smg GDS is likely to be involved in growth arrest and apoptosis coupled with the p53 checkpoint function in mammalian cells.

Rescue of Etoposide-induced Apoptosis by Smg GDS Exogenously Expressed in Smg GDS−/− Thymocytes

To prove Smg GDS deficiency is actually responsible for the apoptotic phenotype in mice, we tried to rescue some of the properties of Smg GDS−/− mice by transducing Smg GDS function. We asked whether expression of the Smg GDS cDNA would overcome apoptosis of Smg GDS−/− thymocytes imposed by etoposide. Accordingly, we isolated primary Smg GDS+/− and Smg GDS−/− thymocytes from newborn mice at the day of birth, transfected them with vectors expressing Smg GDS or EGFP as a control, and further cultured at confluence for the following 24 h. Then cells were treated with etoposide for 4 h to trigger apoptosis; flow cytometry profiles and caspase-3 activity were analyzed as indications of apoptosis. In a representative experiment, percent survival of Smg GDS+/− and Smg GDS−/− thymocytes transfected with an empty vector alone was 61 and 42%, respectively (Figure 7A, left panels). These flow cytometry profiles indicate that Smg GDS−/− thymocytes are more susceptible to etoposide than Smg GDS+/− thymocytes, which is basically consistent with the described results of the caspase-3 assay (Figure 6C). Smg GDS transduction before etoposide treatment, however, increased the percentage of survived Smg GDS−/− thymocytes, both negative for annexin V and propidium iodide, from 42 to 55%, with a reciprocal decrease in apoptotic cells, positive for annexin V and propidium iodide, from 27 to 15% (Figure 7A, lower panels). In contrast, Smg GDS+/− thymocytes transfected with vectors expressing Smg GDS (Figure 7A, upper panels) and EGFP (our unpublished results) did not show significant effects on the percentage of surviving cells, both negative for annexin V and propidium iodide, at similar levels of 61–62%.

Furthermore, rescue of Smg GDS deficiency was seen with caspase-3 activity of Smg GDS−/− thymocytes after the same retroviral challenge (Figure 7B). Transduction of Smg GDS into thymocytes before etoposide treatment lowered the levels of caspase-3 activity, specifically in Smg GDS−/− thymocytes, but not in controls. Mean values of representative cases of five independent experiments are shown. It may reflect inconsistent degrees of apoptotic states in thymocytes in vivo that caspase-3 activity varies according to thymocyte preparations. The caspase-3 assay appeared to be

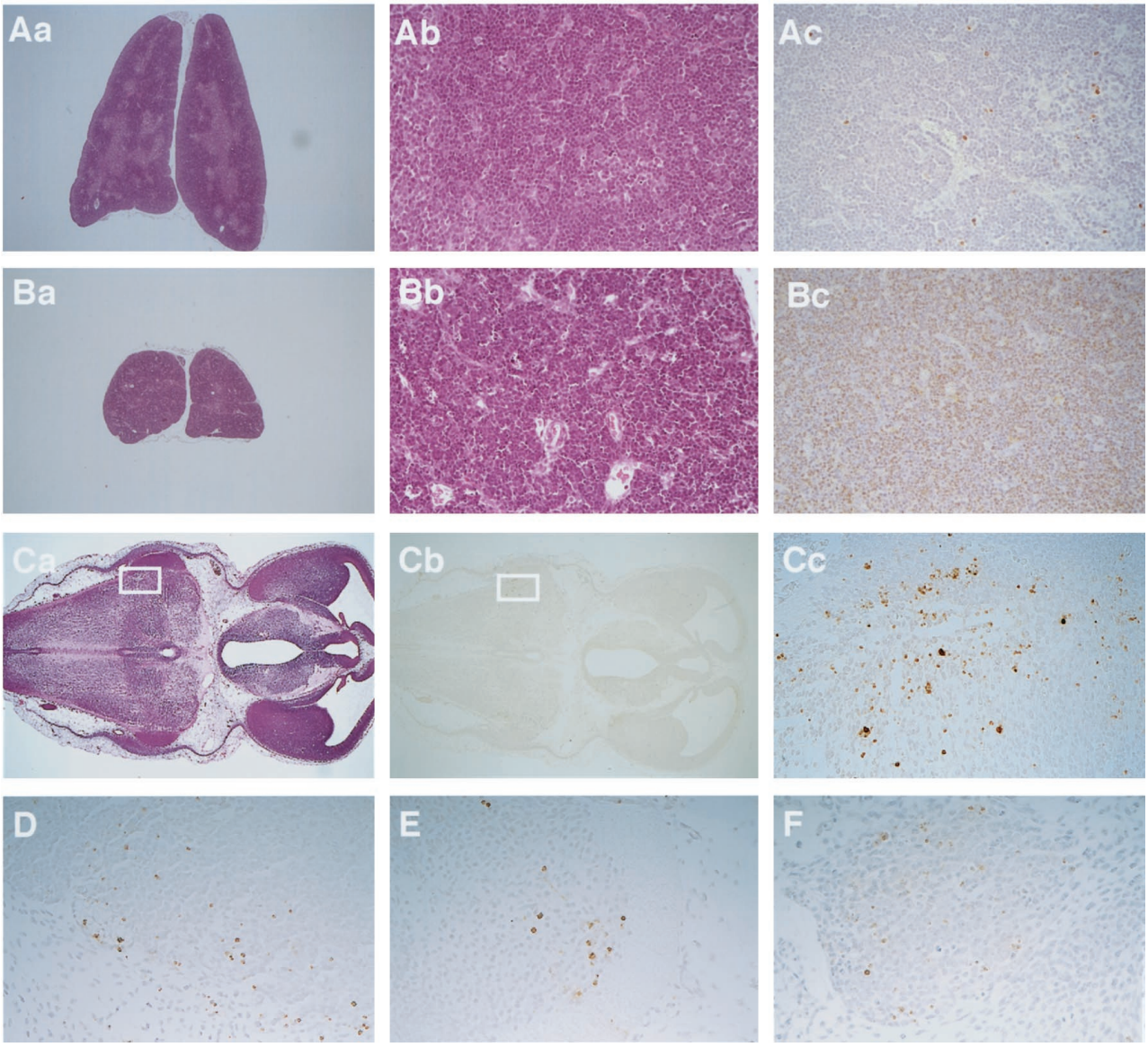

Figure 5. Enhanced apoptosis in the Smg GDS−/− thymus at 1 d after birth and increased neuronal cell death in the Smg GDS−/− embryo. (Aa and Ba) Sections of the wild-type thymus (Aa) and the Smg GDS−/− thymus (Ba) were prepared from littermate mice and stained with HE (20×). The Smg GDS−/− thymus was one-third in size of the wild-type thymus. (Ab and Bb) HE staining of the wild-type thymus (Ab) and the Smg GDS−/− thymus (Bb) at high-power (200×) magnification. Numerous pyknotic nuclei were found in Smg GDS−/− thmocytes compared with the wild-type thymocytes. (Ac and Bc) TUNEL staining of the wild-type thymus (Ac) and the Smg GDS−/− thymus (Bc). TUNEL-positive thymocytes were increased in the Smg GDS−/− thymus. (Ca and Cb) Transverse sections through the third ventricle and the diencephalon of the Smg GDS−/− embryo at 12.5 dpc. (Ca) HE staining of the Smg GDS−/− brain (20×). (Cb) TUNEL staining of the Smg GDS−/− brain (20×). (Cc–F) High-power (200×) magnification. TUNEL-positive neuronal cells were increased in the medulla oblongata (Cc; boxed in Ca and Cb), the trigeminal ganglia (D), the spinal cord (E), and the dorsal root ganglia (F).

more sensitive than the flow cytometry assay to detect the extent of rescue of Smg GDS deficiency. This difference could probably be explained by the observation that the population of apoptotic cells that have already lost caspase-3 activity is excluded in the caspase-3 assay but not in the flow cytometry assay. Because the caspase-3 activity was normalized by the amount of total protein, this assay would reflect the condition of live cells in early apoptotic stages. On the contrary, fluorescence-activated cell sorting includes cells in every apoptotic stage, i.e., even dead cells, which may reduce the sensitivity to detect the effect of Smg GDS transduction. Taken together, these findings suggest that Smg GDS is effective in reducing apoptosis imposed by etoposide.

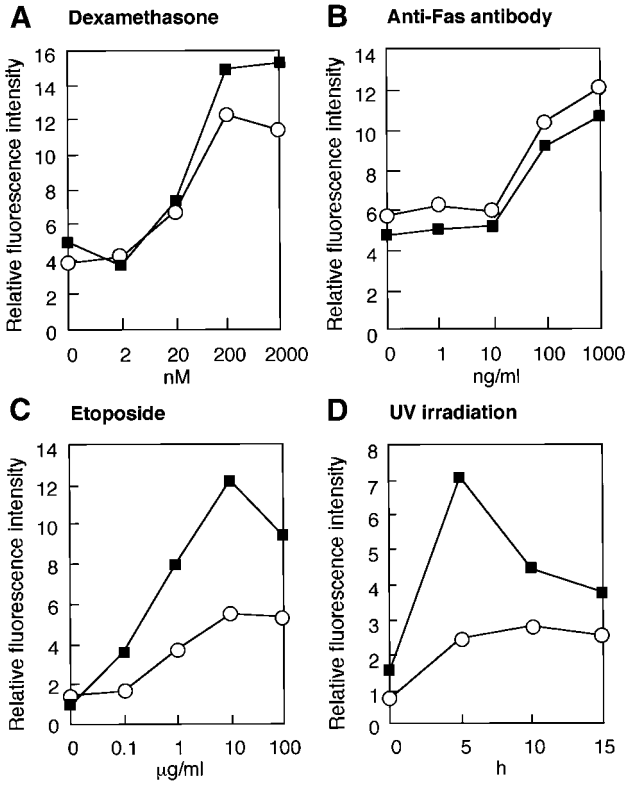

Figure 6. Caspase-3 cleavage activity in defined apoptosis in mouse thymocytes at the day of birth. Mouse thymocytes were treated for 2 h with dexamethasone (A), a mouse Fas monoclonal antibody (B), and etoposide (C) to induce apoptosis at the indicated concentrations. Cells were also treated for the indicated times (h) with UV irradiation (D). Caspase-3 activity was measured as relative fluorescence intensity based on the cleavage of the fluorogenic substrate acetyl-aspartyl-glutamyl-valyl-aspart-1-aldehyde-7-amino-4-trifluoromethyl coumarin. Caspase-3 activities in Smg GDS+/− thymocytes (open circles) and Smg GDS−/− thymocytes (closed squares) are shown. Untreated cells were primarily negative for the presence of active caspase-3.

DISCUSSION

Cooperative Involvement of Environmental Factors and Smg GDS Deficiency in Apoptosis

The pathological mechanism underlying the phenotype of Smg GDS−/− mice appears to be enhanced apoptosis at least in three cell types. Smg GDS deficiency renders the cells susceptible to stimuli that trigger apoptosis, but not all the Smg GDS−/− cells are destined to die. Apoptosis in cardiomyocytes caused heart failure in nearly 70% of Smg GDS−/− newborn mice, whereas 30% of them were still viable. Correspondingly, apoptosis in thymocytes or neuronal cells did not result in overt disorders such as abnormal T-cell maturation or embryonic lethality. Therefore, it is likely that environmental factors trigger apoptosis to generate pathological lesions.

It is important that the neonatal period is the sole critical point in the lifespan of Smg GDS−/− mice. As to Smg GDS−/− cardiomyocytes, the hemodynamic changes during alteration from fetal to systemic circulation are likely to be an environmental stress that triggers apoptosis and culminates in the morphological changes and heart failure. The closure of the ductus arteriosus is known to bring about a sudden increase in left ventricle afterload, which may account for the sudden appearance of apoptotic events in Smg GDS−/− cardiomyocytes. The wild-type heart would normally recover from localized damages, whereas some of Smg GDS−/− hearts would not tolerate these stresses. The notion is consistent with a recent report demonstrating that biomechanical stress triggers cardiomyocyte apoptosis in mice lacking the gp130 cytokine receptor (Hirota *et al.*, 1999). As to Smg GDS−/− thymocytes, possible environmental stresses could be hypoxia caused by heart failure and inappropriate responses to growth or survival signals in vivo. Ex vivo treatment of thymocytes with apoptotic inducers, however, has clearly demonstrated that some genotoxic agents, such as etoposide and UV irradiation, were effective, suggesting the involvement of DNA damage-dependent apoptosis pathway under Smg GDS-deficient conditions. Finally, analysis of the Smg GDS−/− embryos revealed defects only in neuronal development; apoptotic cell death was found in newly generated, postmitotic neurons. Although the biological event triggering Smg GDS−/− neuronal cell death is not readily defined, it is intriguing that deficiency of Smg GDS and Ki-Ras results in similar neuronal developmental defects.

The phenotype of Smg GDS−/− mice can involve proliferative and differentiatve defects except for enhanced apoptosis. However, we have shown that the Smg GDS−/− cardiomyocytes proliferate and differentiate normally as analyzed by BrdU incorporation and by MLC and α-actinin expression. Differentiation of thymocytes was not impaired either when analyzed by flow cytometry using antibodies for CD4 and CD8. Furthermore, primary mouse embryonic fibroblasts lacking Smg GDS show normal proliferative ability in culture; MAPK activity increased to the same level as that of wild-type mouse embryonic fibroblasts when treated with epidermal growth factor (M. Tanaka, unpublished observation). Thus, environmental factors and defects in cell survival signals, but not defects in proliferation and differentiation signals, are likely to cooperate to generate the phenotype of Smg GDS−/− mice.

Molecular Mechanisms of Smg GDS-mediated Survival Signaling In Vivo

Smg GDS is structurally and kinetically different from other GEPs for the Ras and Rap subfamilies (McCrea *et al.*, 1991; Mizuno *et al.*, 1991; Kotani *et al.*, 1992; Kawamura *et al.*, 1993; Orita *et al.*, 1993; Nakanishi *et al.*, 1994). On the basis of biochemical properties, we have proposed the following roles of Smg GDS and Cdc25 on Ki-Ras. Ki-Ras is mainly activated by the action of Cdc25 on the cytoplasmic surface of the plasma membrane. The GTP-bound form of Ki-Ras is then complexed with Smg GDS and transferred to its downstream target molecules, such as c-Raf-1 and B-Raf, from the complex. Once the GTP-bound form of Ki-Ras forms a complex with its target molecules, Smg GDS is dissociated from Ki-Ras and reused for another cycle of translocation of Ki-Ras (Takai *et al.*, 1993).

Although it is not clear which members of the Ras, Rho, and Rap families are natural targets of Smg GDS in vivo,

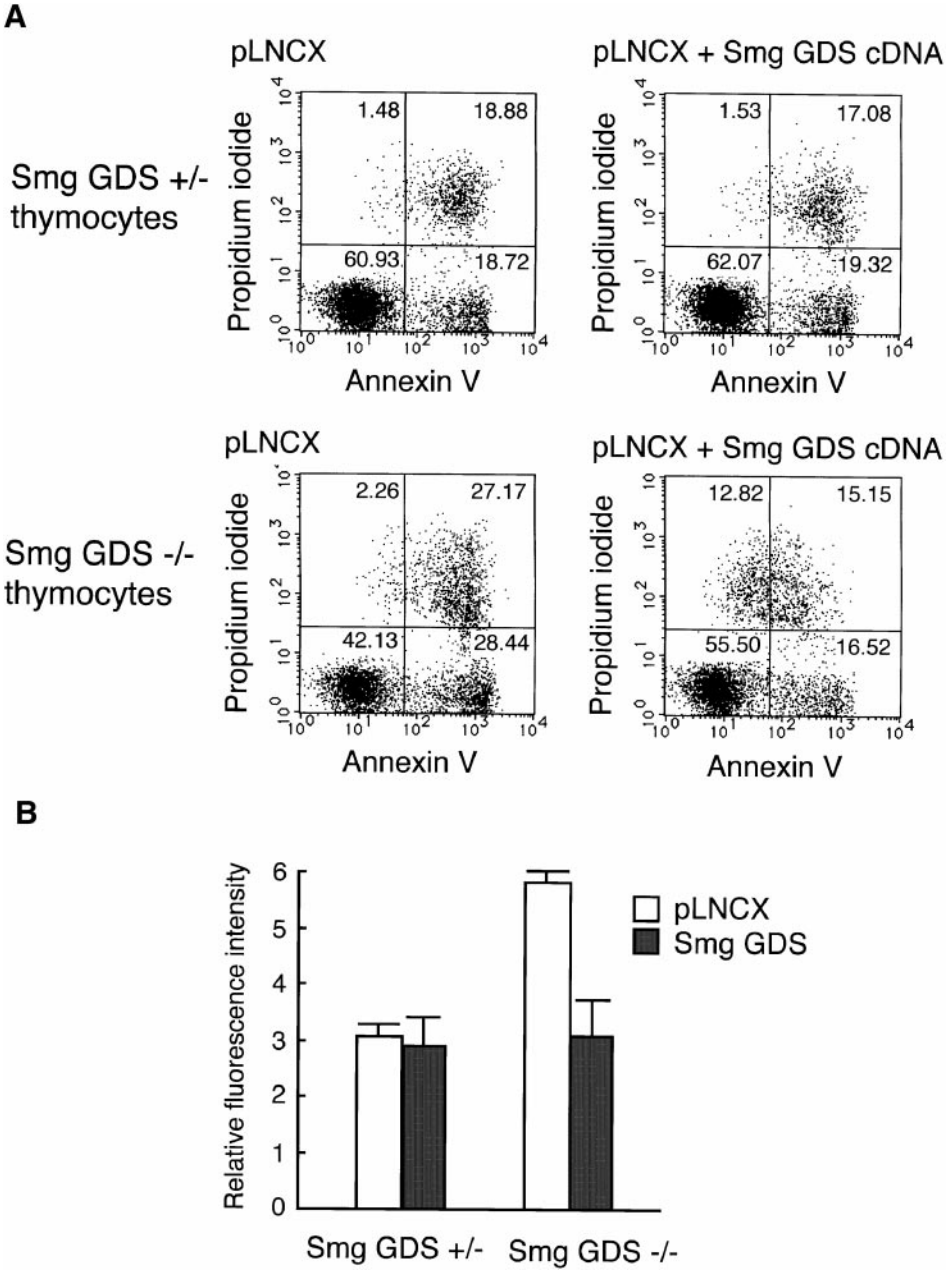

Figure 7. Rescue of etoposide-induced apoptosis by the Smg GDS cDNA exogenously expressed in Smg GDS−/− thymocytes. (A) Cultures of 1×10^6 thymocytes derived from newborn Smg GDS+/− (upper panels) and Smg GDS−/− (lower panels) mice were transduced with empty retroviral vector pLNCX (left panels) and transduced with pLNCX expressing Smg GDS cDNA (right panels). Retrovirus-treated thymocytes were then stimulated for 4 h with etoposide to induce apoptosis, stained with propidium iodide and annexin V-FITC, and analyzed by flow cytometry. The percentage of the total gated cells analyzed is given within the panels. (B) Caspase-3 activity was determined as in Figure 6. Mean values are shown for five independent experiments using Smg GDS+/− and Smg GDS−/− thymocytes after treatment with the empty retroviral vector pLNCX (open boxes) and pLNCX expressing Smg GDS cDNA (shaded boxes) and treatment with etoposide for 4 h.

several clues suggest that Ki-Ras dysfunction is most likely to be involved in generating the phenotype of Smg GDS−/− mice. First, it has recently been reported that Ras1 mediates cell survival signaling in invertebrates (Bergmann *et al.*, 1998b). Biochemically, Ras1 down-regulates the expression of Hid for survival in *Drosophila* (Bergmann *et al.*, 1998a; Kurada and White, 1998). In addition, Ras-mediated phosphatidylinositol 3-kinase inhibits c-*myc*-induced apoptosis (Kauffmann-Zeh *et al.*, 1997), and phosphatidylinositol 3-kinase activates Akt to deliver antiapoptotic signals (Kennedy *et al.*, 1997; Eves *et al.*, 1998). Thus, in mammals, Ki-Ras could be an antiapoptotic transducer that serves to protect the cell from a variety of genotoxic and environmental stresses, including DNA damage, hypoxia, and inappropriate growth signals. Second, there are several similarities between the phenotypes of Smg GDS−/− and Ki-Ras−/− mice. Histopathology of the heart showed the characteristic pattern of hypocellularity in myocardium in both Smg GDS−/− and Ki-Ras−/− mice, and increased neuronal cell death shared the temporal and spatial pattern of distribution in both mutant embryos, although fetal thymocyte development appears normal in Ki-Ras−/− mice. Third, Smg GDS shows GDP/GTP exchange activity only toward Ki-Ras among the three Ras proteins in vitro (Mizuno *et al.*, 1991), whereas knockout mice studies revealed that only Ki-Ras, but not H-Ras and N-Ras, is essentially required for viability

in mice (M. Katsuki, personal communication; Umanoff *et al.*, 1995; Johnson *et al.*, 1997; Koera *et al.*, 1997). Taken together, we presume that Smg GDS deficiency might be a mild form of Ki-Ras deficiency and that the apoptotic phenotype almost certainly results from the absence of a shared Ki-Ras and Smg GDS function.

However, we have not ruled out the possibility that Rho or Rac dysfunction is involved in generating the apoptotic phenotype, especially in the thymi. Survival of thymocytes is impaired in transgenic mice lacking functional Rho by thymic targeting of a transgene encoding C3 transferase from *Clostridium botulinum* (Henning *et al.*, 1997). Recently, inactivation of RhoA, but not Rac1 or Cdc42, has been reported to induce apoptosis in baby hamster kidney cells (Moorman *et al.*, 1999), and Rac1 has been reported to show an antiapoptotic effect in interleukin-3-dependent murine hematopoietic BaF3 cells (Nishida *et al.*, 1999). Therefore, defects in the Smg GDS−/− thymus could be explained by increased apoptosis caused by Rho or Rac dysfunction but not Ras dysfunction. Additionally, an Smg GDS homologue in *Dictyostelium*, named Darlin, has been reported to be necessary for the ability of cells to aggregate in response to starvation but not essential for cytokinesis or development (Vithalani *et al.*, 1998). Because Darlin binds to the glutathione *S*-transferase fusion proteins RacE, RacC, and Cdc42Hs, the interaction of Darlin with the Rho family proteins could be essential for cell survival but not for cell division. Thus, it remains to be determined whether small G proteins other than Ki-Ras actually have antiapoptotic function in mice.

Apoptosis in Smg GDS−/− thymocytes induced by etoposide and UV irradiation suggests the involvement of a DNA damage-dependent apoptosis pathway in the absence of Smg GDS function. DNA damage-dependent apoptosis is evolutionarily well conserved from invertebrates to mammals, compared with Fas-induced apoptosis (Meier and Evan, 1998). Because the role of p53 in DNA damage pathways has been investigated extensively (Harvey *et al.*, 1993; Lowe *et al.*, 1993; Deng *et al.*, 1995; Kamijo *et al.*, 1997), we put forward the hypothesis that cell survival signals stimulate Smg GDS to activate Ki-Ras, and Ki-Ras versus p53 acts as a balance in regulating antiapoptosis and survival and apoptosis signaling.

REFERENCES

Ando, S., *et al*. (1992). Post-translational processing of rac p21s is important both for their interaction with the GDP/GTP exchange proteins and for their activation of NADPH oxidase. J. Biol. Chem. *267*, 25709–25713.

Bergmann, A., Agapite, J., McCall, K., and Steller, H. (1998a). The *Drosophila* gene hid is a direct molecular target of Ras-dependent survival signaling. Cell *95*, 331–341.

Bergmann, A., Agapite, J., and Steller, H. (1998b). Mechanisms and control of programmed cell death in invertebrates. Oncogene *17*, 3215–3223.

Bonfini, L., Karlovich, C.A., Dasgupta, C., and Banerjee, U. (1992). The Son of Sevenless gene product: a putative activator of Ras. Science *255*, 603–606.

Bourne, H.R., Sanders, D.A., and McCormick, F. (1990). The GTPase superfamily: a conserved switch for diverse cell functions. Nature *348*, 125–132.

Bourne, H.R., Sanders, D.A., and McCormick, F. (1991). The GTPase superfamily: conserved structure and molecular mechanism. Nature *349*, 117–127.

Buday, L., and Downward, J. (1993). Epidermal growth factor regulates p21ras through the formation of a complex of receptor, Grb2 adapter protein, and Sos nucleotide exchange factor. Cell *73*, 611–620.

Crechet, J.B., Poullet, P., Mistou, M.Y., Parmeggiani, A., Camonis, J., Boy-Marcotte, E., Damak, F., and Jacquet, M. (1990). Enhancement of the GDP-GTP exchange of RAS proteins by the carboxyl-terminal domain of SCD25. Science *248*, 866–868.

Deng, C., Zhang, P., Harper, J.W., Elledge, S.J., and Leder, P. (1995). Mice lacking p21CIP1/WAF1 undergo normal development, but are defective in G1 checkpoint control. Cell *82*, 675–684.

de Rooij, J., Zwartkruis, F.J., Verheijen, M.H., Cool, R.H., Nijman, S.M., Wittinghofer, A., and Bos, J.L. (1998). Epac is a Rap1 guanine-nucleotide-exchange factor directly activated by cyclic AMP. Nature *396*, 474–477.

Egan, S.E., Giddings, B.W., Brooks, M.W., Buday, L., Sizeland, A.M., and Weinberg, R.A. (1993). Association of Sos Ras exchange protein with Grb2 is implicated in tyrosine kinase signal transduction and transformation. Nature *363*, 45–51.

Enari, M., Sakahira, H., Yokoyama, H., Okawa, K., Iwamatsu, A., and Nagata, S. (1998). A caspase-activated DNase that degrades DNA during apoptosis, and its inhibitor ICAD. Nature *391*, 43–50.

Eves, E.M., Xiong, W., Bellacosa, A., Kennedy, S.G., Tsichlis, P.N., Rosner, M.R., and Hay, N. (1998). Akt, a target of phosphatidylinositol 3-kinase, inhibits apoptosis in a differentiating neuronal cell line. Mol. Cell. Biol. *18*, 2143–2152.

Fujioka, H., Kaibuchi, K., Kishi, K., Yamamoto, T., Kawamura, M. Sakoda, T., Mizuno, T., and Takai, Y. (1992). Transforming and c-fos promoter/enhancer-stimulating activities of a stimulatory GDP/GTP exchange protein for small GTP-binding proteins. J. Biol. Chem. *267*, 926–930.

Fushiki, S., Hyodo-Taguchi, Y., Kinoshita, C., Ishikawa, Y., and Hirobe, T. (1997). Short- and long-term effects of low-dose prenatal X-irradiation in mouse cerebral cortex, with special reference to neuronal migration. Acta Neuropathol. *93*, 443–449.

Gotoh, T., *et al*. (1995). Identification of Rap1 as a target for the Crk SH3 domain-binding guanine nucleotide-releasing factor C3G. Mol. Cell. Biol. *15*, 6746–6753.

Harvey, M., Sands, A.T., Weiss, R.S., Hegi, M.E., Wiseman, R.W., Pantazis, P., Giovanella, B.C., Tainsky, M.A., Bradley, A., and Donehower, L.A. (1993). In vitro growth characteristics of embryo fibroblasts isolated from p53-deficient mice. Oncogene *8*, 2457–2467.

Hall, A. (1990). The cellular functions of small GTP-binding proteins. Science *249*, 635–640.

Henning, S. Galandrini, W.R., Hall, A., and Cantrell, D.A. (1997). The GTPase Rho has a critical regulatory role in thymus development. EMBO J. *16*, 2397–2407.

Hiraoka, K., *et al.* (1992). Both stimulatory and inhibitory GDP/GTP exchange proteins, smg GDS and rho GDI, are active on multiple small GTP-binding proteins. Biochem. Biophys. Res. Commun. *182*, 921–930.

Hirota, H., Chen, J., Betz, U.A.K., Rajewsky, K., Gu, Y., Ross, J., Jr., Muler, W., and Chien, K.R. (1999). Cell survival pathway is a critical event in the onset of heart failure during biomechanical stress. Cell *97*, 189–198.

Hughes, D.A., Fukui, Y., and Yamamoto, M. (1990). Homologous activators of ras in fission and budding yeast. Nature *344*, 355–357.

Johnson, L., *et al*. (1997). K-ras is an essential gene in the mouse with partial functional overlap with N-ras. Genes. Dev. *11*, 2468–2481.

Jones, S., Vignais, M.L., and Broach, J.R. (1991). The CDC25 protein of *Saccharomyces cerevisiae* promotes exchange of guanine nucleotides bound to ras. Mol. Cell. Biol. *11*, 2641–2646.

Kaibuchi, K., Mizuno, T., Fujioka, H., Yamamoto, T., Kishi, K., Fukumoto, Y., Hori, Y., and Takai, Y. (1991). Molecular cloning of the

cDNA for stimulatory GDP/GTP exchange protein for smg p21s (ras p21-like small GTP-binding proteins) and characterization of stimulatory GDP/GTP exchange protein. Mol. Cell. Biol. *11*, 2873–2880.

Kamijo, T., Zindy, F., Roussel, M.F., Quelle, D.E., Downing, J.R., Ashmun, R.A., Grosveld, G., and Sherr, C.J. (1997). Tumor suppression at the mouse INK4a locus mediated by the alternative reading frame product p19ARF. Cell *91*, 649–659.

Kauffmann-Zeh, A., Rodriguez-Viciana, P., Ulrich, E., Gilbert, C., Coffer, P., Downward, J., and Evan, G. (1997). Suppression of c-Myc-induced apoptosis by Ras signaling through PI(3)K and PKB. Nature *385*, 544–548.

Kawamura, M., Kaibuchi, K., Kishi, K., and Takai, Y. (1993). Translocation of Ki-ras p21 between membrane and cytoplasm by smg GDS. Biochem. Biophys. Res. Commun. *190*, 832–841.

Kawasaki, H., Springett, G.M., Mochizuki, N., Toki, S., Matsuda, M., Housman, D.E., and Graybiel, A.M. (1998). A family of cAMP-binding proteins that directly activates rap1. Science *282*, 2275–2279.

Kennedy, S.G., Wagner, A.J., Conzen, S.D., Jordan, J., Bellacosa, A., Tsichlis, P.N., and Hay, N. (1997). The PI3-kinase/Akt signaling pathway delivers an anti-apoptotic signal. Genes. Dev. *11*, 701–713.

Kikuchi, A., Kuroda, S., Sasaki, T., Kotani, K., Hirata, K., Katayama, M., and Takai, Y. (1992). Functional interactions of stimulatory and inhibitory GDP/GTP exchange proteins and their common substrate small GTP-binding protein. J. Biol. Chem. *267*, 14611–14615.

Koera, K., Nakamura, K., Nakao, K., Miyoshi, J., Toyoshima, K., Hatta, T., Otani, H., Aiba, A., and Katsuki, M. (1997). K-ras is essential for the development of the mouse embryo. Oncogene *15*, 1151–1159.

Kotani, K., Kikuchi, A., Doi, K., Kishida, S., Sakoda, T., Kishi, K., and Takai, Y. (1992). The functional domain of the stimulatory GDP/GTP exchange protein (smg GDS) which interacts with the C-terminal geranylgeranylated region of rap1/Krev-1/smg p21. Oncogene *7*, 1699–1704.

Kurada, V., and White, K. (1998). Ras promotes cell survival in *Drosophila* by downregulating hid expression. Cell *95*, 319–329.

Liu, B.X., Wei, W., and Broek, D. (1993). The catalytic domain of the mouse sos1 gene product activates Ras proteins in vivo and in vitro. Oncogene *8*, 3081–3084.

Liu, X., Zou, H., Slaughter, C., and Wang, X. (1997). DFF, a heterodimeric protein that functions downstream of caspase-3 to trigger DNA fragmentation during apoptosis. Cell *89*, 175–184.

Lowe, S.W., Ruley, H.E., Jacks, T., and Housman, D.E. (1993a). p53-dependent apoptosis modulates the cytotoxicity of anti-cancer agents. Cell *74*, 957–967.

Lowe, S.W., Schmitt, E.M., Smith, S.W., Osborne, B.A., and Jacks, T. (1993b). p53 is required for radiation-induced apoptosis in mouse thymocytes. Nature *362*, 847–849.

Lyons, I., Parsons, L.M., Hartley, L., Li, R., Andrews, J.E., Robb, L., and Harvey, R.P. (1995). Myogenic and morphogenetic defects in the heart tubes of murine embryos lacking the homeo box gene Nkx2–5. Genes Dev *9*, 1654–1666.

McCrea, P.D., Turck, C.W., and Gumbiner, B. (1991). A homolog of the armadillo protein in Drosophila (plakoglobin) associated with E-cadherin. Science *254*, 1359–1361.

Meier, P., and Evan, G. (1998). Dying like flies. Cell *95*, 295–298.

Mizuno, T., Kaibuchi, K., Yamamoto, T., Kawamura, M., Sakoda, T., Fujioka, H., Matsuura, Y., and Takai, Y. (1991). A stimulatory GDP/GTP exchange protein for smg p21 is active on the post-translationally processed form of c-Ki-ras p21 and rhoA p21. Proc. Natl. Acad. Sci. USA *88*, 6442–6446.

Moorman, J.P., Luu, D., Wickham, J., Bobak, D.A., and Hahn, C.S. (1999). A balance of signaling by Rho family small GTPases RhoA, Rac1 and Cdc42 coordinates cytoskeletal morphology but not cell survival. Oncogene *18*, 47–57.

Nakanishi, H., Kaibuchi, K., Orita, S., Ueno, N., and Takai, Y. (1994). Different functions of Smg GDS dissociation stimulator and mammalian counterpart of yeast Cdc25. J. Biol. Chem. *269*, 15085–15091.

Nishida, K., Kaziro, Y., and Satoh, T. (1999). Anti-apoptotic function of Rac in hematopoietic cells. Oncogene *18*, 407–415.

Orita, S., Kaibuchi, K., Kuroda, K., Shimizu, K., Nakanishi, H., and Takai, Y. (1993). Comparison of kinetic properties between two mammalian ras p21 GDP/GTP exchange proteins, ras guanine-releasing factor and smg GDP dissociation stimulator. J. Biol. Chem. *268*, 25542–255461.

Simon, M.A., Bowtell, D.D., Dodson, G.S., Laverty, T.R., and Rubin, G.M. (1991). Ras1 and a putative guanine nucleotide exchange factor perform crucial steps in signaling by the sevenless protein tyrosine kinase. Cell *67*, 701–716.

Takai, Y., Kaibuchi, K., Kikuchi, A., and Kawata, M. (1992). Small GTP-binding proteins. Int. Rev. Cytol. *133*, 187–230.

Takai, Y., Kaibuchi, K., Kikuchi, A., Sasaki, T., and Shirataki, H. (1993). Regulators of small GTPases. Ciba Found. Symp. *176*, 128–138.

Togawa, A., *et al*. (1999). Progressive impairment of kidneys and reproductive organs in mice lacking Rho GDIα. Oncogene *18*, 5373–5380.

Umanoff, H., Edelmann, W., Pellicer, A., and Kucherlapati, R. (1995). The murine N-ras gene is not essential for growth and development. Proc. Natl. Acad. Sci. USA *92*, 1709–1713.

Vithalani, K.K., Parent, C.A., Thorn, E.M., Penn, M., Larochelle, D.A., Devreotes, P.N., and De Lozanne, A. (1998). Identification of Darlin, a *Dictyostelium* protein with Armadillo-like repeats that binds to small GTPases and is important for the proper aggregation of developing cells. Mol. Biol. Cell *8*, 3095–3106.

Vojtek, A.B., Hollenberg, S.M., and Cooper, J.A. (1993). Mammalian Ras interacts directly with the serine/threonine kinase Raf. Cell *74*, 205–214.

Walker, F., Kato, A., Gonez, L.J., Hibbs, M.L., Pouliot, N., Levitzki, A., and Burgess, A.W. (1998). Activation of the Ras/mitogen-activated protein kinase pathway by kinase-defective epidermal growth factor receptors results in cell survival but not proliferation. Mol. Cell. Biol. *18*, 7192–7204.

Yaku, H., Sasaki, T., and Takai, Y. (1994). The Dbl oncogene product as a GDP/GTP exchange protein for the Rho family: its properties in comparison with those of Smg GDS. Biochem. Biophys. Res. Commun. *198*, 811–817.

Yamamoto, T., Kaibuchi, K., Mizuno, T., Hiroyoshi, M., Shirataki, H., and Takai, Y. (1990). Purification and characterization from bovine brain cytosol of proteins that regulate the GDP/GTP exchange reaction of smg p21s, ras p21-like GTP-binding proteins. J. Biol. Chem. *265*, 16626–16634.

Yoshida, Y., Kawata, M., Miura, Y., Musha, T., Sasaki, T., Kikuchi, A., and Takai, Y. (1992). Microinjection of smg/rap1/Krev-1 p21 into Swiss 3T3 cells induces DNA synthesis and morphological changes. Mol. Cell. Biol. *12*, 3407–3414.